ELSEVIER

Journal of Nuclear Materials 258–263 (1998) 2008–2012

journal of nuclear materials

Simulation of helium bubble behavior in neutron-irradiated stainless steel during welding

Shohei Kawano *, Rie Sumiya, Koji Fukuya

Power & Industrial Systems R&D Center, Toshiba Corporation, 8 Shinsugita-cho, Isogo-ku, Yokohama 235-8523, Japan

Abstract

A simulation model of helium bubble behavior and crack initiation at grain boundaries in the heat-affected zone (HAZ) during welding is proposed, and the effects of welding conditions and helium concentration on bubble evolution and cracking are evaluated. The model was based on the following assumptions; homogeneous bubble nucleation, bubble coalescence by random motion, bubble growth by vacancy absorption and ductile fracture. The result of calculations for different welding heat inputs reveal that the final bubble size increases with increasing the weld heat input and with decreasing bubble spacing at the grain boundary. The calculated critical heat input for cracking as a function of helium concentration is in good agreement with the results of welding experiments on neutron-irradiated stainless steels and helium-doped stainless steels.

1. Introduction

Large amounts of helium can be produced by (n,α) reactions in the stainless steels subjected to intense neutron exposure. Such stainless steels are known to be susceptible to intergranular cracking in the heat-affected zone (HAZ) during the welding process [1–5]. The mechanism of this cracking is considered to be rapid growth of bubbles formed at grain boundaries under the influence of high temperatures and thermal stresses, to a size sufficient for grain boundary separation. Several investigators have performed welding examinations of neutron-irradiated materials and helium-doped materials in order to understand the weldability and to develop a welding technique suitable for irradiated materials [1–10]. The weldability of helium-containing stainless steels has been found to be influenced by helium concentration and welding conditions such as heat input, weld penetration and constrained condition. A theoretical model of helium bubble growth at grain boundaries has been proposed by Lin et al. [6] and Wang et al. [7], who calculated the effects of thermal history on bubble growth and stress state during welding.

In the present study, a simulation model including helium bubble nucleation, coalescence, growth and resultant cracking in the HAZ during welding is proposed to predict weldability. The effects of welding conditions and helium concentration on weld crack initiation in irradiated materials are evaluated and compared with reported experimental results.

2. Modeling of helium bubble behavior and crack initiation during welding

In order to model helium bubble behavior in irradiated stainless steels during welding, the bubble evolution at grain boundaries is divided into several characteristic stages: bubble nucleation, coalescence, growth and crack occurrence. Fig. 1 shows the stages of bubble evolution and temperature/stress history in the HAZ.

2.1. Bubble nucleation at a grain boundary

Although there have been many experimental and theoretical investigations of bubble nucleation under isothermal annealing conditions, there have been no reports of quantitative data for helium bubble nucleation under post-irradiation welding conditions. Helium atoms in the grains are considered to diffuse and

* Corresponding author. Tel.: +81 45 770 2372; fax: +81 45 770 2483; e-mail: shohei.kawano@toshiba.co.jp.

0022-3115/98/$19.00
PII: S0022-3115(98)00351-1

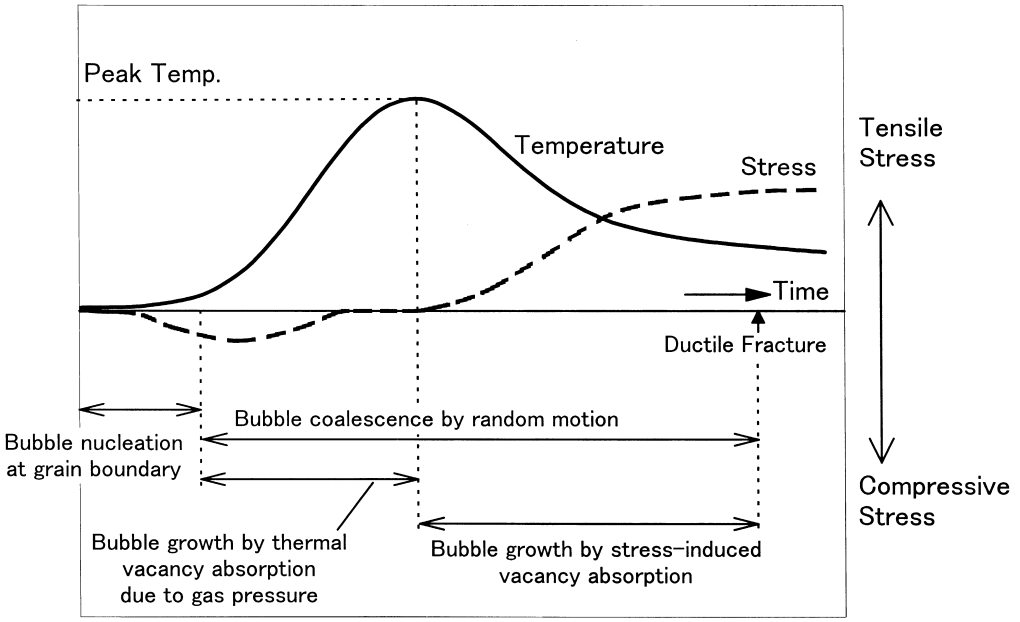

Fig. 1. Modeling of helium bubble behavior during welding.

nucleate bubbles at grain boundaries in the early stages of the heat-up period during welding. Since a high density of defect clusters is produced in grains after neutron irradiation and act as trap sites for helium atoms, only the helium atoms which exist adjacent to grain boundaries are expected to contribute to bubble nucleation at grain boundaries. In the present model, it is assumed that the bubbles nucleate homogeneously at grain boundary and that the areal number density of nucleated bubbles N_0 is proportional to the helium concentration C_{He}, thus

$$N_0 = \alpha C_{He}, \tag{1}$$

where α is a constant.

2.2. Bubble migration and coalescence

At elevated temperatures during welding, the bubble density on grain boundaries decreases due to bubble coalescence along these boundaries [8]. The migration process of bubbles is considered to be random motion controlled by surface diffusion [11]. During this stage, the time rate of change of the bubble density (N) is given [12] by

$$\frac{dN}{dt} = \frac{2\pi D_b N^2}{\ln(L/4r)}, \tag{2}$$

where the bubble spacing $L = 1/\sqrt{N}$ and the bubble diffusion coefficient $D_b = D_s (a/r)^4$ (where D_s is the surface diffusion coefficient, r the bubble radius and a the lattice spacing).

The average radius of a coalesced bubble r_c is assumed to be regarded as obeying the conservation of volume

$$r_c = r_1 (N_1/N_c)^{1/3}, \tag{3}$$

where r_1 and N_1 denote the radius and density of bubbles before coalescence, respectively and N_c is the density of coalesced bubble.

2.3. Bubble growth in the heat-up period

In the heat-up period, bubbles grow by thermal vacancy absorption due to helium gas overpressure in the bubble [6]. The growth rate of the bubble is given by

$$\frac{dr}{dt} = \frac{\delta \Omega D_{gb} C_v^e}{2r^2}, \tag{4}$$

where δ is the grain boundary thickness, Ω the atomic volume, D_{gb} the self-diffusion coefficient in the grain boundary and C_v^e the equilibrium vacancy concentration. Bubble growth and coalescence in the heat-up period are assumed to occur at temperatures above 923 K, considering the experimental results that the growth and coalescence of helium bubbles become observable by transmission electron microscopy (TEM) after annealing at temperatures above 923 K for 1 h in irradiated stainless steel with 100 atomic parts per million (appm) He [13].

2.4. Bubble growth in the cooling period

In the cooling period, the bubble growth is caused by stress-induced vacancy absorption [6]. The growth rate

of grain boundary bubbles under tensile stress is derived from the creep void growth mechanism [14]

$$\frac{dr}{dt} = \frac{2\pi\delta\Omega D_{gb}\sigma}{LrkT}, \quad (5)$$

where σ is the tensile stress normal to the grain boundary and k Boltzmann's constant. The tensile stress (σ) is simulated by using elasticity theory [6]: $\sigma = E\,\alpha_l\,[T_{max} - T]$, where E is the Young's modulus, α_l the thermal expansion coefficient and T_{max} the peak temperature during welding. The stress is specified as $\sigma = 200$ MPa when calculated σ exceeds 200 MPa, considering the plastic deformation that will occur.

2.5. Cracking at grain boundaries

The morphology of a weld crack is known to be ductile fracture on grain boundaries decorating a dimple structure [2,5,6]. In the present model, bubbles at grain boundaries are assumed to act as cavities or voids in micromechanism models of ductile fracture. It is also assumed that cracking occurs when the tensile strain imposed in the HAZ exceeds the fracture strain (ε_f) calculated by the following equation according to Mclintock's ductile fracture model [15]

$$\varepsilon_f = \frac{(1-n)\,\ln(L/2r)}{\sinh\left[\sqrt{3}(1-n)/2\right]}, \quad (6)$$

where n is the work hardening rate. The tensile strain imposed in the HAZ is simply deduced from the volume change induced by weld metal shrinkage.

2.6. Calculation

The bubble diameter in the HAZ during welding was calculated for different heat input conditions assuming single bead-on-plate welds by the gas tungsten arc (GTA) process. The temperature–time relationship during welding was derived from heat conduction analysis in an infinite solid with a moving point heat source. The diameter and density of bubbles was obtained by iterative calculation of Eqs. (2)–(5). The parametric values used in the calculation are shown in Table 1.

3. Calculational results and discussion

Fig. 2 shows the temperature and helium bubble diameter as a function of time for different weld heat inputs at 0.1 mm from the fusion line, where the HAZ cracking has been observed in helium-containing stainless steels [6]. The growth rate of the helium bubble is enhanced at higher heat input, since the temperature in the HAZ is raised for longer periods by increasing the heat input. Fig. 3 shows the effect of heat input on final bubble size for the different initial bubble spacing together with the critical weld heat input for cracking. The final bubble diameter increases with increasing weld heat input and decreasing initial bubble spacing. On the other hand, as the initial bubble spacing becomes higher, the critical weld heat input for cracking becomes higher. Fig. 4 shows the final bubble diameter and spacing as a function of the distance from the fusion line welded at 1 kJ/cm heat input. The increase in the size and spacing of bubbles is restricted to the narrow region that extends only 1 mm below the fusion line. This result agrees with the bubble microstructure observed by TEM after low-penetration welding in helium-doped stainless steels with 85 appm He [8].

The critical weld heat input for cracking as a function of the helium concentration can be derived from the results in Fig. 3 and Eq. (1). Fig. 5 shows the calculated criteria for cracking in a helium concentration vs. heat input map assuming $\alpha = 1.25 \times 10^{12}$ (m^{-2} $appm^{-1}$) in Eq. (1) together with the results of welding experiments

Table 1
Parameter values used in calculation

Initial bubble radius r_0	1 nm
Grain boundary thickness δ	0.4 nm
Atomic volume Ω	1×10^{-29} m^3
Lattice spacing a	0.2 nm
Self-diffusion coefficient in the GB D_{gb} [16]	2×10^{-4} exp(−1.65 eV/kT) m^2/s
Surface diffusion coefficient D_s [17]	0.4·exp(−2.2 eV/kT) m^2/s
Equilibrium vacancy concentration C_v^e [6]	$C_v^e = [\exp(\Delta S_v/k)\exp(-\Delta H_v/kT)]/\Omega$ m^{-3}
Boltzmann's constant k	8.618×10^{-5} eV/K
Vacancy formation entropy ΔS_v	1.5 k
Vacancy formation energy ΔH_v	1.8 eV
Work hardening rate n	0.3
Thermal expansion coefficient α_l [18]	2×10^{-5} K^{-1}
Young's modulus E [19]	$[243.9 - 0.1078\ T] \times 10^9$ N/m^2
Initial bubble spacing L_0	50–2000 nm
Weld heat input Q	1–15 kJ/cm

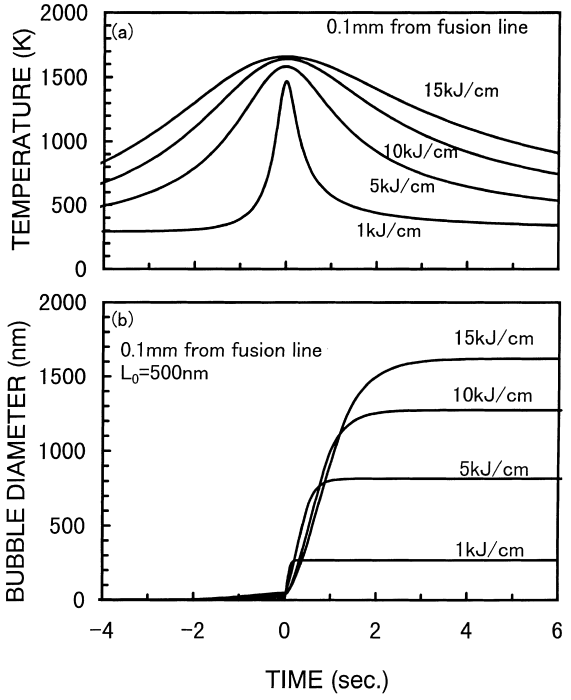

Fig. 2. Temperature (a) and helium bubble diameter (b) as a function of time for different welding heat inputs.

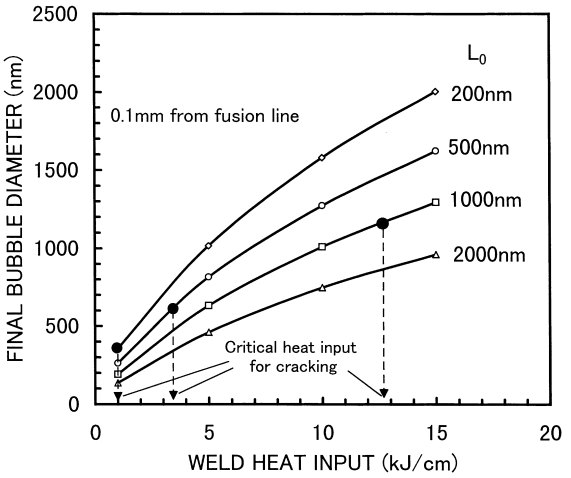

Fig. 3. Final bubble diameter as a function of welding heat input for different initial bubble spacing L_0. Solid circles indicate the critical weld heat input for cracking calculated by Eq. (6).

[5,9]. The calculated criterion for cracking is in good agreement with the result of the welding experiment. For $\alpha = 1.25 \times 10^{12}$, the final bubble spacing is 0.9 μm in the case of welding at 1 kJ/cm for 1 appm He. This spacing is consistent with the dimple spacing of about 1 μm

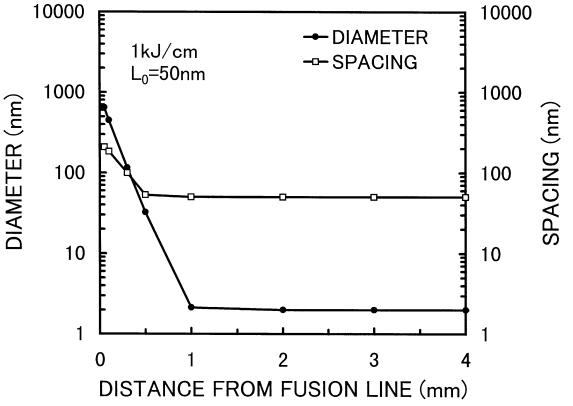

Fig. 4. The final bubble diameter and spacing as a function of the distance from fusion line in the case of welding at 1 kJ/cm.

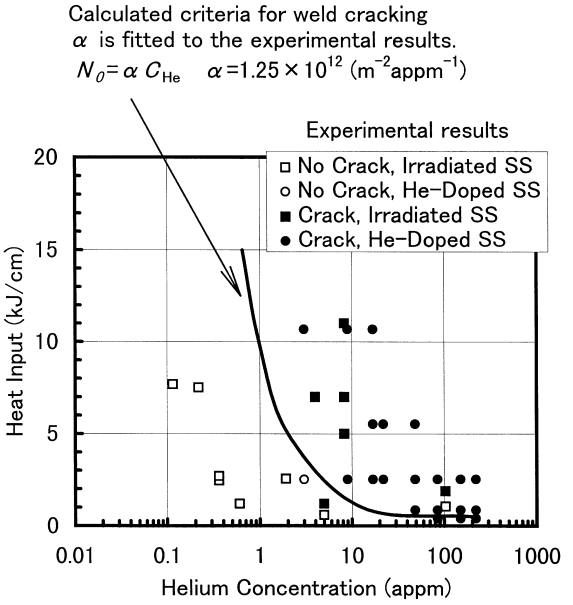

Fig. 5. Comparison of the calculated cracking criteria with results of welding experiments for neutron-irradiated stainless steels and helium-doped stainless steels [5,9].

observed on the HAZ fracture surface after GTA welding at 0.7 kJ/cm in helium-doped stainless steels containing 2.5 appm He [6]. Hence, the present simulation model has good capability for predicting weldability.

The constant α in the present model is an adjustable parameter for the experimental data. To determine a reasonable value of α and to improve modeling of the nucleation stage of helium bubbles, details of the bubble morphology in welded helium-containing materials are necessary.

4. Summary

Helium bubble nucleation, growth and crack occurrence in HAZ during welding were modeled and the effects of welding conditions and helium concentration on cracking were evaluated. The result of calculations for different welding heat inputs revealed that the final bubble size increases with increasing weld heat input and with decreasing bubble spacing at a grain boundary. The calculated critical heat input for cracking as a function of helium concentration was in good agreement with the results of welding experiments on neutron-irradiated stainless steels and helium-containing stainless steels.

References

[1] W.R. Kanne Jr., Weld. J. August (1988) 33.
[2] W.R. Kanne Jr. et al., J. Nucl. Mater. 225 (1995) 69.
[3] C.A. Wang et al., J. Nucl. Mater. 239 (1996) 85.
[4] K. Watanabe et al., Fusion Eng. Design 31 (1996) 9.
[5] K. Asano et al., J. Nucl. Mater., submitted.
[6] H.T. Lin, M.L. Grossbeck, B.A. Chin, Metal. Trans. A 21 (1990) 2585.
[7] C.A. Wang, M.L. Grossbeck, B.A. Chin, J. Nucl. Mater. 225 (1995) 59.
[8] S.H. Goods, N.Y.C. Yang, Metal. Trans. A 23 (1992) 1021.
[9] E.A. Franco-Ferreira, W.R. Kanne Jr., Weld. J. February (1992) 43.
[10] S. Kawano et al., these Proceedings.
[11] A. Ryazanov et al., J. Nucl. Mater. 233–237 (1996) 1076.
[12] D.R. Olander, Fundamental aspects of nuclear reactor fuel elements, Energy Research and Development Administration, USA, 1976, p. 215.
[13] Y. Ishiyama et al., J. Nucl. Mater. 239 (1996) 90.
[14] D. Hull, D.E. Rimmer, Philos. Mag. 4 (1959) 673.
[15] F.A. McClintock, J. Appl. Mech. June (1968) 363.
[16] D.W. James, G.M. Leak, Philos. Mag. 12 (1965) 491.
[17] L.A. Gilifalco, Atomic Migration in Crystals, Japanese edition, Kyoritu, Tokyo, 1980, p. 188.
[18] M. Mochizuki et al., Nucl. Eng. Design 144 (1993) 439.
[19] A. Sather, J. Acoust. Soc. Am. 43 (6) (1968) 1291.